

# Surface Structural Techniques Applied to Interfaces

I.K. Robinson

## Introduction

An interface is an internal surface, the boundary between two media which may be crystalline, amorphous solid, or liquid. Its close similarity with a surface, a solid-vacuum boundary, suggests that many of the powerful techniques available for studying surfaces might be applied to the interface structure problem. The extent to which this is possible is the subject of this article.

The techniques to be discussed in this article include low energy electron diffraction (LEED), medium energy ion scattering (MEIS), x-ray diffraction, and x-ray reflectivity. (The most widely used method, transmission electron microscopy (TEM), is the subject of a separate article in this issue of the *MRS BULLETIN*.) To summarize what we will find, surface methods were developed to be nonpenetrating in order to have surface sensitivity. This works against us in the interface situation by requiring the use of extremely thin samples, at least on one side of the interface. This means special handling of samples in some cases and raises the possibility of artificial results. Of the three methods, x-ray diffraction is the most penetrating and least surface sensitive; it probably has the greatest potential for widespread use in interface science.

This article defines structure as "atomic structure" for this purpose: we are interested in the coordinates of atoms at the interface and their relation to bulk structures on one or both sides. For this reason, we will consider only interfaces that are crystalline on at least one side. Since crystals are by far our strongest structural reference point, much less can be said about other interfaces. We will also consider the morphology of an interface, defined as the boundary of the crystal(s) that demarcates the interface, also at the

atomic level. This is most apparent in the form of interface roughness. The roles of strain and misfit dislocations in interface formation, also studied by these techniques, are outside the scope of this article.

## Low Energy Electron Diffraction (LEED)

LEED is a classic example of a technique that has been adapted and optimized for surfaces. First demonstrated by Davisson and Germer,<sup>1</sup> it utilizes the wave properties of the electron to undergo diffraction from a crystal; matching the wavelength to the atomic spacing requires using electrons in the 5–500 eV energy range. Since electrons of this energy interact very strongly with matter, the penetration is limited to about 10 Å, and so the measurements are intrinsically surface sensitive. Otherwise, the structural and morphological information is contained in the angular distribution of the diffraction intensity, which can be measured accurately and modeled reasonably with a dynamical calculation.<sup>2</sup> The limited penetration is, however, a problem for an interface that is more than 10 Å inside a material. Henzler and colleagues<sup>3</sup> developed a method of chemically processing Si/SiO<sub>2</sub> interfaces to remove the oxide and expose the bare Si crystal morphology to the vacuum, thus rendering them suitable for analysis by LEED.

What is learned about these interfaces concerns not so much the atomic arrangement, which is probably perturbed by the HF etching,<sup>3</sup> but the distribution of steps on the surface. The presence of steps implies that an interface is rough, and the roughness is quantified by the spatial distribution of steps. This information is contained in the reciprocal

space distribution of intensity around each of the diffraction peaks. For this reason, the technique is called spot-profile analysis, or SPA-LEED. To do a good job, well-collimated electron beams must be used to obtain high resolution. An example is shown in Figure 1, taken from the published work of Henzler's group in Hannover.<sup>4</sup>

Because only 10 Å of crystal is penetrated, the shape of the electron diffraction pattern in reciprocal space is elongated into continuous rods oriented perpendicular to the surface (interface). Along these rods at regular intervals lie the Bragg peaks of the bulk crystal, at which every atom scatters in-phase to give a maximum in the intensity (ignoring dynamical effects for now). Exactly halfway between these positions, alternate layers of the crystal scatter 180° out-of-phase with each other, so if a step is present the terraces on either side destructively interfere with each other and lead to broadening of the peak in the plane perpendicular to the rod. The width of the peak is then inversely related to the size of the terrace (i.e., to the spacing of the steps.) Furthermore, the distribution of intensity across the rod is related (via Fourier transformation) to the distribution of steps.

The scans of Figure 1 were made through the reciprocal space position (11/2, 11/2, 11/2), exactly satisfying this out-of-phase condition along the specular rod of the (111)-oriented substrate. The solid curve in Figure 1a is for a well-annealed, clean Si(111) wafer. It shows only a sharp Gaussian-shaped peak that represents the instrument-response (resolution) function. There are no steps on this surface within the coherence length of the instrument, about 140 Å here. The broad experimental curve is for a stripped Si(111)/SiO<sub>2</sub> interface and shows considerable detail. In the analysis,<sup>4</sup> a total of four components is considered:

1. A constant flat background. This arises from point defects and thermal diffuse scattering.
2. The resolution-limited central peak. This comes from the flat regions of the surface. This component's height does vary between the in-phase and out-of-phase positions, implying a slight roughness of 1.44 Å rms.
3. A narrow Lorentzian-shaped peak also attributed to roughness of the interface. A geometric distribution of steps (constant step probability per site in one dimension) with a characteristic separa-

## Surface Structural Techniques Applied to Interfaces

tion of 37 Å would give rise to this component. This is not present around the Bragg peak, since all atoms are in-phase there.

4. A broad Lorentzian-shaped peak clearly separated from the narrow one in the fitting. This is found to be present around the in-phase Bragg peaks as well, so it is not related to steps or roughness. Rather, it must come from small coplanar patches within the surface that have a different scattering power from Si. The average size of these patches, given by the reciprocal of the peak width, is 9 Å or three atomic spacings. Their composition is not uniquely determined, but it is suggested that they may be oxide clusters within the top Si layer.<sup>4</sup> They might also come from stacking-faulted patches similar to those seen in the 7×7 reconstruction of Si(111).

Upon annealing the previously stripped samples, the first three components were found to change little, while component 4 was reduced dramatically.<sup>4</sup>

## X-Ray Diffraction

The basic principles of x-ray diffraction from interfaces are even simpler than for electron diffraction because the kinematic approximation is generally applicable. For x-ray wavelengths about 1 Å and relatively light materials, penetration is limited by photoelectric absorption to a depth of microns, provided the grazing angle regime is avoided. Thus, to a reasonable approximation for interfaces within ~1000 Å of an accessible surface, there is no penetration problem, and the diffraction from an interface can be seen superimposed on that of the bulk surrounding it. Needless to say, that bulk contribution is far from negligible because it arises from a far greater amount of material.

The advantage of x-rays, particularly those produced by electron storage rings at facilities such as the National Synchrotron Light Source (NSLS) at Brookhaven National Laboratory, is their very high resolution. The typical resolution function of a three-axis diffractometer fills only  $5 \times 10^{-10}$  of the Brillouin zone of Si. The bulk diffraction is localized in pointlike Bragg peaks, smaller than this resolution element. Scattering from point defects and bulk thermal diffuse scattering (TDS) are diffuse in all reciprocal space directions. Only the surfaces and interfaces, by virtue of their two-dimensional translational symmetry, give rise to rodlike lines of scattering; everything else can

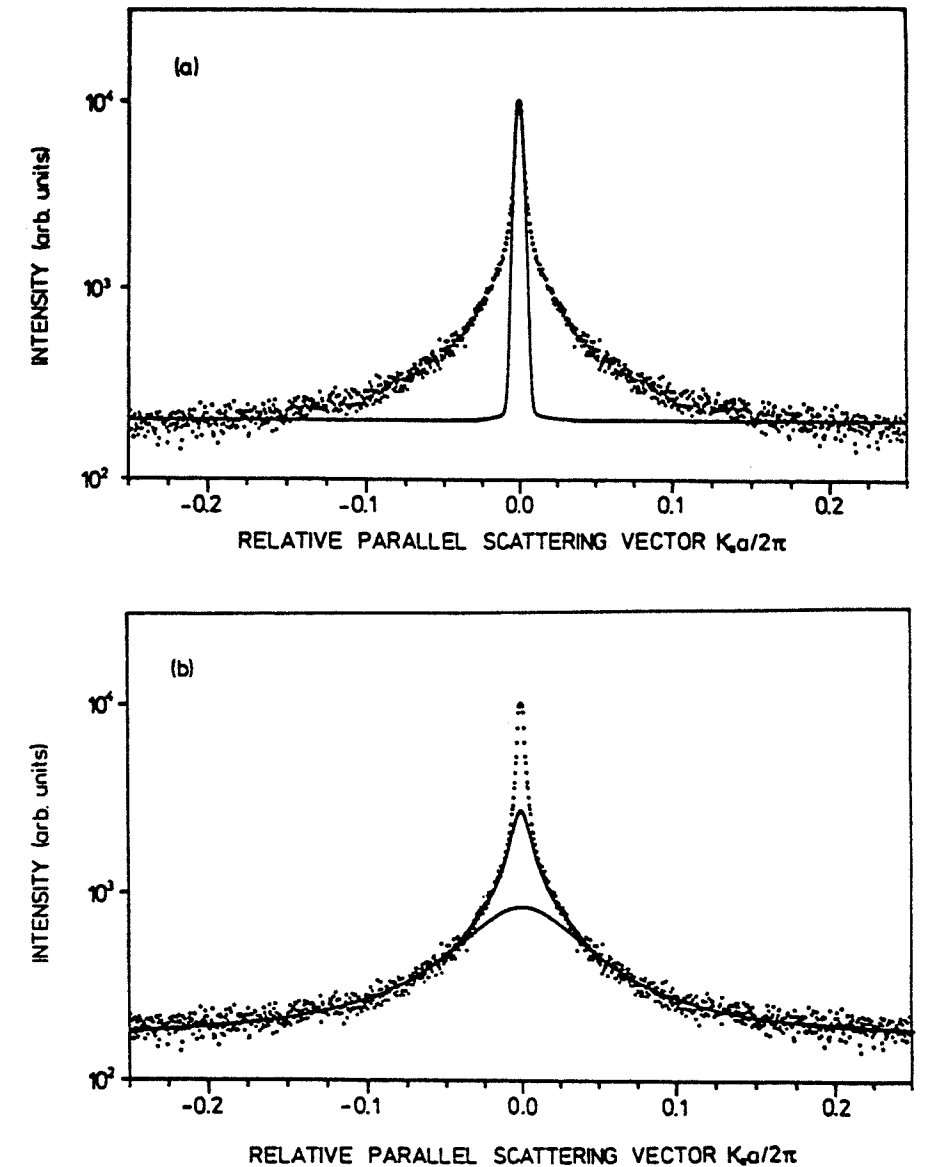


Figure 1. Low energy electron diffraction (LEED) measurement of the intensity profile across the specular diffraction rod of a chemically stripped Si(111)/SiO<sub>2</sub> interface. (From Reference 4 with permission.)

be filtered out either by avoidance (3D Bragg peaks) or by background subtraction (diffuse scattering). Distinguishing the buried interface from the surface through which it is measured is then the only outstanding problem.

The overall situation is not quite the same for the crystal/amorphous and the crystal/crystal interface, so we will consider an example of each.

## Crystal/Amorphous Interface

For a direct comparison with the LEED study above, we show x-ray dif-

fraction intensity data for the Si(111)/SiO<sub>2</sub> interface<sup>5</sup> in Figure 2. The data are filtered in the manner previously described, so they correspond to diffraction from this interface alone. Since the SiO<sub>2</sub> film is amorphous, there is also no crystalline contribution to the CTR from the external surface. The broken curve is the calculated crystal truncation rod<sup>6</sup> (CTR) of a Si crystal terminating with an ideal Si(111) bilayer. CTRs are the x-ray equivalent of the continuous rods seen in LEED, but they have orders of magnitude more modulation because the

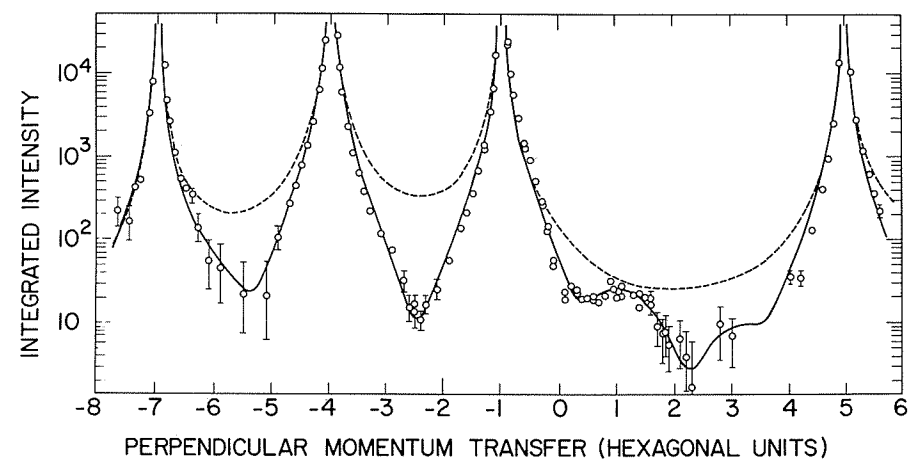


Figure 2. X-ray measurement of the first-order crystal truncation rod (CTR) of the Si(111)/SiO<sub>2</sub> interface. Each point is the integrated intensity of a rocking scan with the diffuse background subtracted. Four bulk peaks are intersected where the CTR diverges, but these are not measured and would be far off-scale. (From Reference 5.)

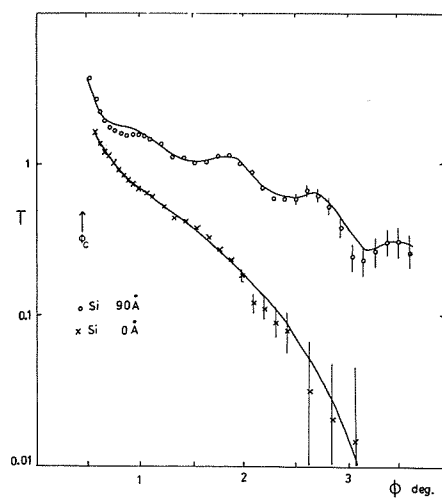


Figure 3. X-ray reflectivity (multiplied by  $\phi^4$ ) as a function of incidence angle for two Si(111)/SiO<sub>2</sub> interfaces. Film A was grown to have a thickness of 90 Å; film B is a native oxide obtained by stripping and exposure to air. (From Reference 7 with permission.)

penetration is so much greater. As stated previously, alternate layers scatter out-of-phase midway between the Bragg peaks. The observation is most sensitive to steps there, just where Figure 2 shows the biggest deviations. The solid curve includes an atomic model of the interface that adds three half bilayers of Si with partial occu-

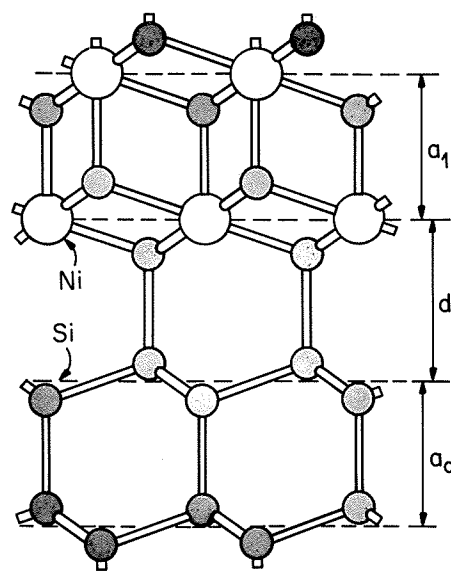


Figure 4. Ball and stick model of the B-type Si(111)/NiSi<sub>2</sub> interface.

pancy<sup>5</sup> and leads to an extremely good fit. The rms height deviation of this model<sup>5</sup> is 1.53 Å, in excellent agreement with LEED.<sup>4</sup> No information was obtained about the lateral distribution of the steps; this would come from measurements analogous to those of Figure 1.

Other x-ray measurements of the

Si(111)/SiO<sub>2</sub> interface have been made. Cowley and Ryan<sup>7</sup> measured the zero-order CTR on the side of the (111) Bragg peak for a variety of different thin oxides. They found almost ideal  $|q|^{-2}$  dependence of the intensity in all cases, using data spanning momentum transfer deviations,  $|q|$ , up to 0.4 in the units of Figure 2. This implies an rms roughness of  $0 \pm 2$  Å, which is within error of the values obtained above.<sup>4,5</sup> According to Figure 2, the slightly rough surface (solid curve) does deviate from the ideal (broken) noticeably by  $|q| = 0.4$ , but this is asymmetric about the Bragg peaks because of a slight contraction within each of the Si(111) bilayers.<sup>5</sup> An asymmetry has also been detected by Harada and Kashiwagura<sup>8</sup> in similar measurements of CTRs from the Si(111)/SiO<sub>2</sub> interface.

### X-Ray Reflectivity

Cowley and Ryan<sup>7</sup> also measured the x-ray reflectivity of their Si(111)/SiO<sub>2</sub> samples. This technique is complementary to diffraction because there is no automatic differentiation between crystalline and noncrystalline materials, since the total momentum transfer is close to zero: it is the electron density profile that is probed directly. For this reason, both the surface and interface of the Si(111)/SiO<sub>2</sub> samples are observed together, and clear oscillations of the reflected intensity as a function of  $|q|$  are therefore seen from their mutual interference. The data are shown in Figure 3.

A multiparameter model is used to fit the reflectivity, which is found to be sensitive to the thickness and density of the oxide and the roughness of both boundaries. Since the air/SiO<sub>2</sub> surface has a much bigger density step than the Si(111)/SiO<sub>2</sub> interface, the fit is more sensitive to surface than interfacial roughness. The rms values obtained for the interface were  $0 \pm 0.2$  Å and  $0 \pm 1.0$  Å for samples A and B, respectively.<sup>7</sup> This measurement is outside the range of values quoted previously, but the quoted error bar<sup>7</sup> is probably rather optimistic.

### Crystal/Crystal Interface

The second example, the B-type Si(111)/NiSi<sub>2</sub> interface, is shown schematically in Figure 4. The lattice mismatch between Si and NiSi<sub>2</sub> is extremely small, 0.005 at room temperature and smaller still at the elevated temperatures of its growth. When a sufficiently thin film of NiSi<sub>2</sub> is grown on Si, it undergoes a slight hexagonal distortion so that the in-plane parameters match

exactly. The critical film thickness, below which the distortion takes place, is many hundreds of angstroms. Figure 4 shows the known structure (see below) of the interface with coordination number 7 at the Ni. Other configurations might be constructed, for example, with one less layer of Si and the interfacial bonds linking directly to the Ni. These ultimately result in a different value of the parameter  $d$ , which is the fundamental structural parameter. A complete description of the structure would also include the strain fields on each side, which might extend several layers deep.

Diffraction from a crystal/crystal interface is necessarily different because both crystals contribute: there is a CTR from the thick (i.e., semi-infinite) substrate and a finite-size-limited Bragg peak from the thin film, which is also a streak of continuous scattering diffuse in the direction perpendicular to the film. Since the lateral lattice parameters are matched, these rods superimpose. And since the film is adjacent to the substrate, the diffraction amplitudes must interfere in a way that is critically dependent on the separation, which is the structural parameter  $d$ . Other details are important too: the choice of termination at each side, the strain fields, the lateral registry, the roughness of the outer surface, etc. Analysis of the intensity along the rod can determine all of these, in principle.

The measured intensity<sup>9</sup> along the rod in the vicinity of the (111) Bragg peak is shown in Figure 5. The peak is clearly asymmetric. The respective contributions of the substrate CTR and the thin film are drawn as labeled, broken curves. The number of layers was determined by the node spacing to be an admixture of 7 and 8 layers. These curves are individually symmetric about their centers, but the amplitude superposition yields a strong asymmetry because (1)  $d$  is greater than the lattice spacing, and (2)  $a_1$  is smaller than  $a_0$ , leading to a slight difference in the center positions. The combined fit shown leads to an accurate determination<sup>9</sup> of both  $d$  and  $a_1$ . The interface is contracted by  $0.08 \pm 0.06$  Å from the configuration of ideal bond lengths (which would give  $d = 9/8$ ). The roughness of the outer surface was found to be negligible for this particular sample.

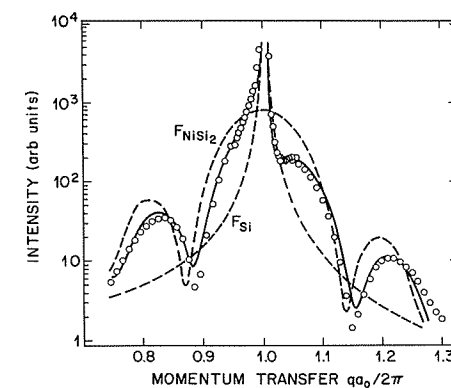


Figure 5. X-ray diffraction intensity profile of the rod passing through the Si(111) Bragg peak of the Si(111)/NiSi<sub>2</sub> interface. (Adapted from Reference 9.)

### Medium Energy Ion Scattering (MEIS)

The last technique to be discussed in this incomplete survey is MEIS, which has also been applied to the Si(111)/NiSi<sub>2</sub> interface.<sup>10</sup> The channeling of protons of suitable energies is well known to occur along the major crystallographic directions of crystals. The strong interaction makes the scattering slightly inelastic and allows the identification (by energy analysis) of the scattering depth of each proton detected. A clear peak in the energy spectrum is thereby seen for channeling along the (001) direction of a NiSi<sub>2</sub> film, which arises from additional material at the Si(111)/NiSi<sub>2</sub> interface.<sup>10</sup> This is due to substrate atoms effectively blocking the channel (see Figure 4). Computer simulations show that for sufficiently thin films, there is a strong correlation between the angle of incidence to the channel and the spatial position of the beam within the channel when it reaches the interface. Thus the beam may be focused to some extent onto the atoms of the substrate, whose positions are therefore revealed.

Van Loenen et al.<sup>10</sup> used this not only to prove the seven-fold coordination model of Figure 4 but also to determine the parameter  $d$  to some accuracy. The value obtained corresponds to a contraction of the interface with respect to the ideal geometry of  $0.06 \pm 0.08$  Å, comparing favorably with the later x-ray

measurement.<sup>9</sup> The most accurate determination of  $d$  comes from the x-ray standing wave technique, giving contractions of  $0.11 \pm 0.03$  Å<sup>11</sup> and  $0.06 \pm 0.03$  Å<sup>12</sup> for the two experiments on films of very different thickness.

The general applicability of MEIS to interface structure is limited first to crystal/crystal interfaces, so that channeling can be caused. The focusing effect is a very subtle one and is only likely to give definitive results when the substrate atoms substantially block the channels of the thin film, as in the case of the B-type Si(111)/NiSi<sub>2</sub> interface, where the stacking order of the planes is reversed.

### Acknowledgments

This article was written while the author was on leave at the Université de Grenoble. The data of Figures 2 and 5 were taken at the Stanford Synchrotron Radiation Laboratory (SSRL), which is supported by the U.S. Department of Energy's Office of Basic Energy Sciences and by the National Institutes of Health Biotechnology Resource Program.

### References

1. C.J. Davisson and L.H. Germer, *Phys. Rev.* **30** (1927) p. 705.
2. M.A. van Hove and S.Y. Tong, *Surface Crystallography by Low Energy Electron Diffraction* (Springer, Berlin, 1979).
3. P.O. Hahn and M. Henzler, *J. Appl. Phys.* **52** (1981) p. 4122.
4. J. Wollschläger and M. Henzler, *Phys. Rev. B* **39** (1989) p. 6052.
5. I.K. Robinson, W.K. Waskiewicz, R. Tung, and J. Bohr, *Phys. Rev. Lett.* **57** (1986) p. 2714.
6. S.R. Andrews and R.A. Cowley, *J. Phys. C* **18** (1985) p. 6427; I.K. Robinson, *Phys. Rev. B* **33** (1986) p. 3830.
7. R.A. Cowley and T. Ryan, *J. Phys. D* **20** (1987) p. 61.
8. J. Harada and N. Kashiwagura, *Colloque de Physique* **50** (1989) p. C7-129.
9. I.K. Robinson, R.T. Tung, R. Feidenhans'l, *Phys. Rev. B* **38** (1988) p. 3632.
10. E.J. van Loenen, J.W.M. Frenken, J.F. van der Veen, and S. Valeri, *Phys. Rev. Lett.* **54** (1985) p. 827.
11. E. Vlieg, A.E.M.J. Fischer, J.F. van der Veen, B.N. Dev, and G. Materlik, *Surf. Sci.* **178** (1986) p. 36.
12. J. Zegenhagen, K.G. Huang, W.M. Gibson, B.D. Hunt, and L.J. Schowalter, *Phys. Rev. B* **39** (1989) p. 254. □